JOURNAL OF GUIDANCE, CONTROL, AND DYNAMICS
Vol. 22, No. 6, November–December 1999

Attitude Commands Avoiding Bright Objects and Maintaining Communication with Ground Station

Hari B. Hablani*
The Boeing Company, Downey, California 90242-2693

The objective of the paper is to develop attitude commands for slewing a vehicle such that the angle of its boresight with the centroid of a bright object is not less than a minimum angle and its antennae do not lose communication with the ground. These commands involve three angles: the required pitch/yaw slew angle, the bright object's exclusion angle normal to the slew angle, and a roll angle for maintaining communication. The location of the bright object's centroid is formulated in terms of an angle normal to the ideal slew plane. If the ideal, minimum-angle slew path enters the forbidden perimeter around the bright object, two alternative exclusion angles are determined so as to pass the object tangentially from either side. Between the two angles, that exclusion angle is selected, which steers the ground station trace, in the communication beam, toward beam axis and not away from it. Communication links of the antennae are maintained by rolling the vehicle before, during, or after slewing. The three-axis attitude and rate commands are illustrated for a stressing scenario in which two bright objects are close by and hence pose special circumstances for the algorithm to tackle.

I. Introduction

SPACECRAFT, whether Earth-pointing, inertially stabilized, or interplanetary, and exoatmospheric interceptors are sometimes required to slew from one direction in space to another in such a way that, en route, the sensitive payloads do not see bright objects such as the sun, moon, and Earth, and that antennae do not lose communication with the ground. This paper is concerned with devising attitude commands for these purposes. The subject of the attitude maneuvers avoiding certain directions in space has been considered in the past. Following robotics science,[1] McInnes[2–4] utilized a composite function consisting of a harmonic potential and constraint potentials, the former having the global minimum at the desired final attitude and the latter generating vortex velocity fields centered at forbidden directions. Perhaps novel and ingenious, this procedure nonetheless seems irrelevant for the present application because the examples in Refs. 1–4 reveal that a telescope, while being slewed, moves toward, instead of away from, the avoidance cone and when near the cone, the telescope slides aimlessly around it unless incidentally pulled over by the global potential function. Thus, though the telescope boresight does avoid the forbidden directions, it meanders substantially away from its nominal path. Sorenson,[5] on the other hand, uses an approach based on spacecraft orbit geometry, relative motion of the sun around the Earth, and varying Earth disc diameter for an elliptic orbit. He formulates pointing constraints that minimize the heat input from the sun to a cryogenically cooled telescope by applying differential geometry to determine possible attitude paths. Singh et al.[6] developed a constraint monitor algorithm to protect sensors of Cassini spacecraft from viewing the sun. Frakes et al.[7] devised a velocity avoidance algorithm to protect the heavy ion large telescope instrument boresight from hazardous debris in the neighborhood of the spacecraft orbit. The algorithm maintains a minimum of a 90-deg ram angle of the boresight with the spacecraft velocity vector. It is the vectorial kinematics approach of Refs. 5–7 that is called upon in this paper.

Whereas the exclusion/communication algorithm developed in the paper generates time-varying attitude and angular rate commands, one may instead use, for simplicity, step commands. For example, Fig. 1a illustrates a minimum-angle slew path AB of a sensor starting from its initial orientation A to its final orientation B. En route, the sensor crosses the sun. To avoid this crossing, the sensor is step-commanded first to turn to the point C or to the opposite point D on the disc (the selection contingent upon the communication requirements). After arriving there, the sensor is step-commanded to the final orientation B. This approach is simple in that the attitude controller receives two sequential step commands, and therefore the associated flight software is compact. However, the disadvantage of this approach is that if the path ADB or ACB taken by the sensor enters the disc, depending on the location $(\alpha^*, \varepsilon^*)$ of the disc's centroid relative to the initial and final orientation of the sensor, this incursion will be neither detected nor averted by the flight controller. To redress this, the step commands may be devised more judiciously as shown in Fig. 1b (the disc's centroid in Fig. 1b lies, for simplicity, on the ideal slew path AB, $\varepsilon^* = 0$). Now, the forbidden area around the bright disc is enlarged so that, ignoring transients, the sensor will traverse the path ADB where AD and DB are tangential to the earlier forbidden area. The sensor is thus step-commanded to the orientation D, and, after arriving there and stopping, it is step-commanded next to its final orientation B. The intermediate orientation D can be determined analytically or numerically. Depending on the flight controller and actuators (wheels, thrusters), the actual path of the sensor in these two illustrations might differ significantly from the expected path ADB. For one thing, because of the step commands, the controller must stop and restart the sensor at D, which is wasteful. More important, because the slew angle α and the exclusion angle ε are about arbitrary axes in the pitch/yaw plane of the vehicle, they cause a coupled multi-axis motion. As a result, the actual path of the sensor may not be as well-behaved as what it will be if the flight controller receives reference α and ε command profiles from A to B and three-axis body rate commands involving $\dot{\alpha}$ and $\dot{\varepsilon}$. For this reason, the paper develops such reference commands.

The contents of the paper are briefly summarized now. Section II formulates various aspects of attitude motion for a bright object avoidance. The parameters of a minimum-angle slew, namely, slew angle, slew axis, and its orientation relative to both the initial vehicle frame and the final boresight direction, are determined first. The coordinates α^*, ε^* of the centroid of a bright object relative to the ideal slew plane are determined next. Then follows the determination of the two opposite exclusion angles (Fig. 1a) about an axis in the pitch/yaw plane, each enabling the telescope to pass the forbidden disc around a bright object tangentially at $\alpha = \alpha^*$. While the slew angle α is varied as a time/fuel-optimal profile, the exclusion angle ε varies as a versine function of α, reaching the desired avoidance angle at the slew angle $\alpha = \alpha^*$. Should this $\varepsilon(\alpha)$ profile intersect the disc for a certain range of α, this versine segment is replaced by the corresponding arc of the forbidden circle around the bright

Received 15 July 1998; revision received 15 March 1999; accepted for publication 27 April 1999.

*Principal Engineering Specialist, Avionics Engineering, Flight Control Systems, Reusable Space Systems, Boeing North America. Associate Fellow AIAA.

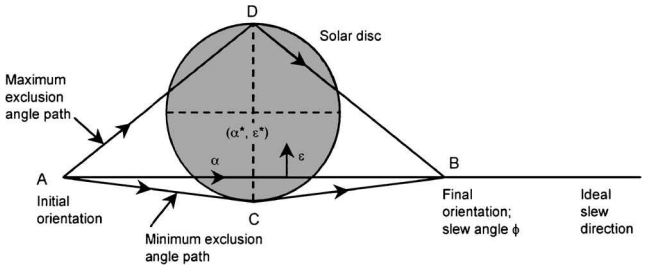

Fig. 1a Step commands producing exclusion paths that cross the sun.

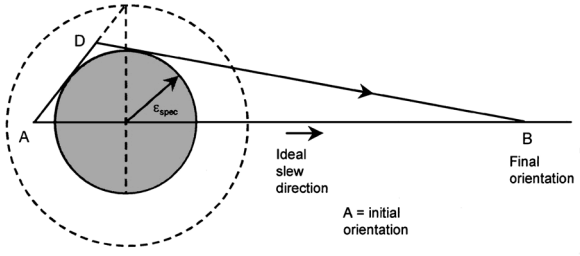

Fig. 1b Ideal tangential exclusion path to avoid the sun using step commands.

object. The formulation for this replacement is developed in this section. Sections III and IV deal with the roll motions required for communication maintenance of the antennae with ground station. For antennae with their communication cones along pitch and yaw axes, a roll motion restores the communication if the geometry of the vehicle location, ground station location, and the communication beam size permit it at all. For $-x$ antenna a roll motion prior to the slew is formulated so as to keep the ground station within the conical beam of the antenna for the complete slew maneuver. This preroll motion, however, cannot always maintain communication if the ground-station projection happens to lie in a forbidden region. On the other hand, the two opposite exclusion angles determined in Sec. II are such that one turns the antenna beam axis away from the ground station while the other turns toward it, the former exclusion angle being clearly undesirable whereas the latter is desirable. The conditions to identify them so are devised in Sec. V. The time-varying angular rate commands associated with slew, exclusion, and roll motion for communication are furnished in Sec. VI. Finally, these attitude and rate commands are illustrated in Sec. VII in the context of an exoatmospheric vehicle, and the paper is concluded in Sec. VIII.

II. Bright Object Avoidance: Formulation

Ideal Slew

Figure 2 portrays the line-of-sight (LOS) unit vector $\boldsymbol{\ell}_0$ along the initial direction of the boresight and $\boldsymbol{\ell}_f$ along its final desired direction. The figure depicts a bright object s to be avoided by the telescope. The most natural axis of rotation to slew the telescope from $\boldsymbol{\ell}_0$ to $\boldsymbol{\ell}_f$ is normal to the plane containing these two noncollinear unit vectors. Denote the unit vector along this axis of rotation as $\boldsymbol{b}$ and the angle between $\boldsymbol{\ell}_0$ and $\boldsymbol{\ell}_f$ as ϕ. Then

$$\sin\phi = |\boldsymbol{\ell}_0 \times \boldsymbol{\ell}_f|, \qquad 0 < \phi < \pi \tag{1}$$

$$\mathbf{b} = \frac{\boldsymbol{\ell}_0 \times \boldsymbol{\ell}_f}{\sin\phi} \tag{2}$$

To complete the definition of the right-handed triad associated with the unit vectors $\boldsymbol{\ell}_0$ and $\boldsymbol{b}$, define a unit vector $\boldsymbol{a}$ in the plane $\boldsymbol{\ell}_0 - \boldsymbol{\ell}_f$ such that $\boldsymbol{a} = \boldsymbol{b} \times \boldsymbol{\ell}_0$. The coordinate frame associated with the triad $\boldsymbol{\ell}_0\, \boldsymbol{a}\, \boldsymbol{b}$ (in this sequence) is denoted $x'_{b0}\ y'_{b0}\ z'_{b0}$ where the subscript b denotes the spacecraft body, 0 denotes the initial orientation of the spacecraft, and the prime distinguishes it from the initial spacecraft frame $x_{b0}\ y_{b0}\ z_{b0}$: $x_{b0} = x'_{b0}$, and the axes y_{b0}, z_{b0} related to y'_{b0}, z'_{b0} through a roll angle γ (Fig. 3). Because the initial LOS unit vector $\boldsymbol{\ell}_0$ is along the boresight axis x_{b0}, the components of $\boldsymbol{\ell}_0$ in the initial

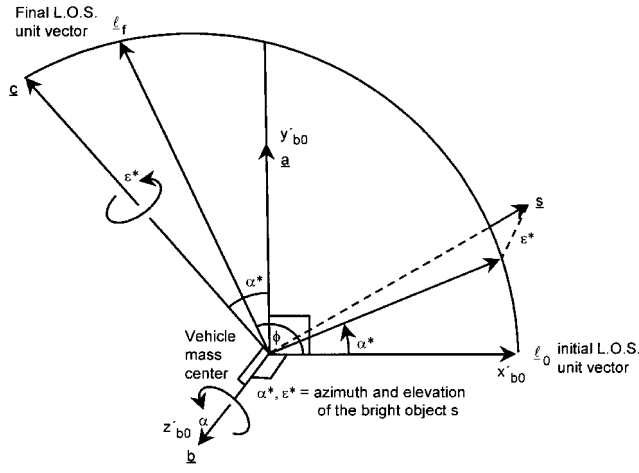

Fig. 2 Location of a celestial object relative to the ideal slew plane of the boresight.

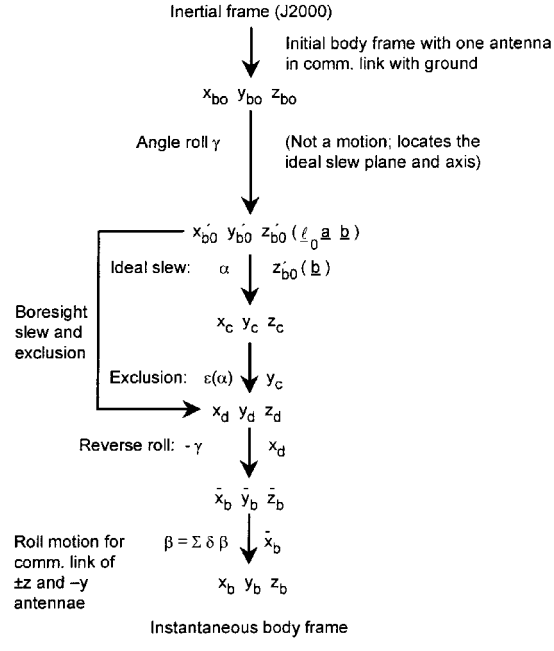

Fig. 3 Various coordinate frames required for boresight slew and communication maintenance of $-y$ and $\pm z$ antennae.

frame $\mathcal{F}^{b0}$: $x_{b0}\ y_{b0}\ z_{b0}$ are $\boldsymbol{\ell}_0 = [1\ \ 0\ \ 0]^T$. Moreover, the unit vectors $\boldsymbol{a}$ (y'_{b0}) and $\boldsymbol{b}$ (z'_{b0}), both being normal to $\boldsymbol{\ell}_0$, are in the pitch-yaw (yz) plane, inclined at a roll angle γ with y_{b0} and z_{b0}, respectively. Therefore,

$$\tan\gamma = \frac{\boldsymbol{\ell}_f \cdot \boldsymbol{b}_{30}}{\boldsymbol{\ell}_f \cdot \boldsymbol{b}_{20}} \tag{3}$$

where the unit vector $\boldsymbol{b}_{20}$ is along y_{b0} axis and $\boldsymbol{b}_{30}$ along z_{b0}. Because the components $\boldsymbol{\ell}_f \cdot \boldsymbol{b}_{20}$ and $\boldsymbol{\ell}_f \cdot \boldsymbol{b}_{30}$ are known, the angle γ can be calculated.

Exclusion Angles

As shown earlier in Fig. 1a, the centroid of the bright object s is specified by an angle (called azimuth here) α^* in the slew plane $\boldsymbol{\ell}_0 - \boldsymbol{\ell}_f$ (or $x'_{b0}\ y'_{b0}$) about the axis $\boldsymbol{b}$ and an elevation angle ε^* about the once-displaced axis y'_{b0} (the unit vector $\boldsymbol{c}$ in Fig. 2). The unit vector $\boldsymbol{s}$ pointing to the center of the celestial object s (s from the sun) can be expressed in the frame $\boldsymbol{\ell}_0\, \boldsymbol{a}\, \boldsymbol{b}$, thus

$$\boldsymbol{s} = \boldsymbol{s} \cdot \boldsymbol{\ell}_0\, \boldsymbol{\ell}_0 + \boldsymbol{s} \cdot \boldsymbol{a}\, \boldsymbol{a} + \boldsymbol{s} \cdot \boldsymbol{b}\boldsymbol{b} \tag{4}$$

the three components being known because the unit vectors $\boldsymbol{s}$, $\boldsymbol{\ell}_0$, $\boldsymbol{\ell}_f$ and therefore $\boldsymbol{a}$ and $\boldsymbol{b}$ are all known in an inertial frame, J2000

for example. Furthermore, using the angles α^*, ε^*, $\boldsymbol{s}$ is expressed in the frame $\boldsymbol{\ell}_0\ \boldsymbol{a}\ \boldsymbol{b}$ as (Fig. 3)

$$\boldsymbol{s} = c\varepsilon^* c\alpha^*\, \boldsymbol{\ell}_0 + c\varepsilon^*\, s\alpha^*\, \boldsymbol{a} - s\varepsilon^*\, \boldsymbol{b} \tag{5}$$

where $s(\cdot) = \sin(\cdot)$ and $c(\cdot) = \cos(\cdot)$. Comparing the three components in Eqs. (4) and (5), the angles α^* and ε^* are found to be

$$\alpha^* = \tan^{-1}[(\boldsymbol{s}\cdot\boldsymbol{a}), (\boldsymbol{s}\cdot\boldsymbol{\ell}_0)], \qquad -\pi \le \alpha^* \le \pi \tag{6}$$

$$\varepsilon^* = -\sin^{-1}(\boldsymbol{s}\cdot\boldsymbol{b}), \qquad -\pi/2 < \varepsilon^* < \pi/2 \tag{7}$$

provided $-\pi/2 < \varepsilon^* < \pi/2$ so that $c\varepsilon^* > 0$.

A bright object is considered for avoidance when, loosely speaking, $0 \le \alpha^* \le \phi$. This condition is not exact for the following reason. A celestial object is to be avoided by a minimum specified angle denoted $\varepsilon_{\text{spec}}$ (Fig. 1b); that is, there is a disc of radius $\varepsilon_{\text{spec}}$ around the celestial object centered at $(\alpha^*, \varepsilon^*)$ that the boresight must not enter. For $\varepsilon^* = 0$ the extreme azimuth angles of the disc boundary will then be $\alpha^* \pm \varepsilon_{\text{spec}}$, and for the disc to be considered for avoidance the azimuth angle α^* must satisfy the exact condition: $-\varepsilon_{\text{spec}} \le \alpha^* \le \phi + \varepsilon_{\text{spec}}$. But, usually, mission planning will ensure that the initial and final orientations of the sensor boresight are not within the $\varepsilon_{\text{spec}}$ radius of a bright object. In any event, for simplicity, we will continue to use the loose condition stated earlier. For a bright object within $0 \le \alpha^* \le \phi$, the minimum deviation angle $\varepsilon_{\min}$ required for avoiding this object is determined as follows. Figure 4 illustrates two celestial objects, one with $\varepsilon^* > 0$ and the other with $\varepsilon^* < 0$. The illustration shows that the ideal slew path of the boresight (the azimuth, α, axis in Fig. 4) about the axis $\boldsymbol{b}$ will intersect the $\varepsilon_{\text{spec}}$ disc if $|\varepsilon^*| < \varepsilon_{\text{spec}}$, and then for the boresight to avoid entering the disc, $\varepsilon_{\min}$ at $\alpha = \alpha^*$ must be

$$\varepsilon_{\min} = \begin{cases} -\text{sign}\big(\varepsilon_{\text{spec}} - |\varepsilon^*|, \varepsilon^*\big) & \text{if} \quad |\varepsilon^*| < \varepsilon_{\text{spec}} \quad (8a) \\ 0 & \text{if} \quad |\varepsilon^*| > \varepsilon_{\text{spec}} \quad (8b) \end{cases}$$

In subsequent sections we will see that sometimes the sign of $\varepsilon_{\min}$ is such that the avoidance motion ε causes the antenna to turn away from the ground station and possibly break the communication link. In that event $\varepsilon_{\min}$ must be replaced by the maximum value

$$\varepsilon_{\max} = \text{sign}\big(\varepsilon_{\text{spec}} + |\varepsilon^*|, \varepsilon^*\big) \quad \text{if} \quad |\varepsilon^*| < \varepsilon_{\text{spec}} \tag{9}$$

to pass the disc tangentially from the opposite side. This will align the antenna more with the ground station. Furthermore, when two or more bright objects are close together or overlap (sunrise, sunset, moonrise, moonset, sun and moon in the neighborhood—although the moon will not be full bright then), the minimum or maximum deviation angles prescribed by Eqs. (8) and (9) may not be able to prevent the boresight from entering the disc of a neighboring celestial object. Ad hoc solutions for such special circumstances are presented in one of the early versions of this paper.[8]

The discrete angles (α^*, $\varepsilon_{\min}$ or $\varepsilon_{\max}$) could be used to construct step commands discussed in the Introduction. But, if one desires to input a reference command profile to the attitude controller, the slew angle α must be expressed as a function of time and ε as a function of α. For this purpose an $\varepsilon(\alpha)$ profile is composed, piecing together discrete exclusion angles for the centroids of different bright objects that cross the ideal slew path and the initial and final exclusion angles (if not zero) at zero and final slew angles. Note that the initial and final exclusion angles are zero unless a bright object covers the initial or final direction of the sensor. Because a versine ($1 - \cos\theta$ type) profile has zero slope at the beginning and at the end and can be shaped to be tangential to a disc at its centroidal angle α^*, this profile is used here as an $\varepsilon(\alpha)$. One such profile and its slope, satisfying the boundary conditions $\varepsilon = \varepsilon_i$ at $\alpha = \alpha_i$ and $\varepsilon = \varepsilon_{i+1}$ at $\alpha = \alpha_{i+1}$ is (α_i and α_{i+1} are the centroidal slew angles of the discs i and $i+1$, respectively)

$$\varepsilon = \tfrac{1}{2}(\varepsilon_i + \varepsilon_{i+1}) - \tfrac{1}{2}(\varepsilon_{i+1} - \varepsilon_i)\cos\eta \tag{10}$$

$$\frac{\mathrm{d}\varepsilon}{\mathrm{d}\alpha} = \frac{\pi}{2}\frac{\varepsilon_{i+1} - \varepsilon_i}{\alpha_{i+1} - \alpha_i}\sin\eta \tag{11}$$

$$\eta = \frac{\alpha - \alpha_i}{\alpha_{i+1} - \alpha_i}\pi \tag{12}$$

These relations can be specialized for $\varepsilon_i = 0$ at $\alpha_i = 0$, or $\varepsilon_{i+1} = 0$ at α_{i+1} = the final slew angle ϕ, or for any other special circumstance. Also the rate $\dot{\varepsilon}$ is calculated from $\dot{\varepsilon} = (\mathrm{d}\varepsilon/\mathrm{d}\alpha)\dot{\alpha}$ where $\dot{\alpha}$ is equal to the instantaneous slew rate determined from a time/fuel optimal slew profile of α.

Forbidden Disc Entry

Depending on the location and size of the disc relative to the slew path, the ε profile [Eq. (10)] may cause the sensor to enter a bright disc when the slew angle α is $\alpha_i < \alpha < \alpha_{i+1}$. In that instance this $\varepsilon(\alpha)$ is replaced by an $\varepsilon(\alpha)$ that commands the sensor to slide along the disc perimeter. According to spherical geometry, the equation of a small disc boundary of radius $\varepsilon_{\text{spec}}$, centered at $(\alpha^*, \varepsilon^*)$, in terms of the coordinates (α, ε) of the points on the circular boundary is

$$c\varepsilon\ c\varepsilon^*\, c(\alpha - \alpha^*) + s\varepsilon\, s\varepsilon^* = c\varepsilon_{\text{spec}} \tag{13}$$

At the slew angles α_1 and α_2, where the ideal slew path intersects the disc (Fig. 4), the avoidance angles ε are zero by definition. Hence, substituting $\varepsilon = 0$ into Eq. (13), we arrive at

$$\varepsilon = 0: c(\alpha_{1,2} - \alpha^*) = \frac{c\varepsilon_{\text{spec}}}{c\varepsilon^*} \tag{14}$$

which furnishes the angles $\alpha_1 < \alpha^*$ and $\alpha_2 > \alpha^*$. The boresight's entry of the forbidden area is checked within the range $\alpha_1 < \alpha < \alpha_2$ as follows.

If a point (α, ε) of the versine profile is within a disc, the angle between (α, ε) direction and $(\alpha^*, \varepsilon^*)$ direction will be less than $\varepsilon_{\text{spec}}$, and, therefore, according to Eq. (13),

$$\text{boresight entered the disc} \Leftrightarrow c\varepsilon\ c\varepsilon^*\, c(\alpha - \alpha^*) + s\varepsilon\, s\varepsilon^* > c\varepsilon_{\text{spec}} \tag{15}$$

If this condition is not satisfied, the boresight is outside the disc. Thus, if the commanded orientation (α, ε) of the next sample satisfies the preceding inequality, the boresight will be inadvertently commanded to enter the disc unless this ε is replaced by a perimeter ε for the same slew angle. The perimeter ε may be obtained by solving the transcendental Eq. (13) for a given $(\alpha - \alpha^*)$ angle using the Newton–Raphson technique, by substituting $\varepsilon = \varepsilon^* + \delta\varepsilon$ and expanding $s\varepsilon$ and $c\varepsilon$ up to the second order of $\delta\varepsilon$. Alternatively, define a frame $x_d^*\ y_d^*\ z_d^*$ analogous to the frame $x_d\ y_d\ z_d$ (which is defined in Fig. 3) arrived at after the rotation $\alpha = \alpha^*$ and $\varepsilon = \varepsilon^*$. Then, the disc perimeter may be expressed parametrically in terms

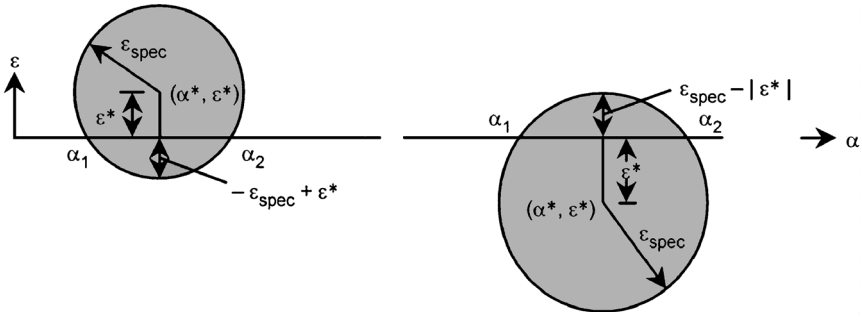

Fig. 4 Minimum deviation angles required for avoiding a celestial object.

of an angle θ $(-\pi \le \theta \le \pi)$ measured from the y_d^* axis in the disc plane. The boresight x_b can be oriented in a direction (α, ε) on the disc boundary by an angle of rotation $\Delta\alpha$ about the z_d^* axis and $\Delta\varepsilon$ about the $\Delta\alpha$-displaced y_d^* axis. Expressing then the boresight unit vector in the frame $x_d^*\ y_d^*\ z_d^*$, Ref. 8 shows that

$$\tan\Delta\alpha = c\theta \tan\varepsilon_{\text{spec}} \tag{16}$$

$$s\Delta\varepsilon = -s\varepsilon_{\text{spec}} s\theta \tag{17}$$

To determine the boundary angle ε corresponding to the slew angle α $(\alpha_1 < \alpha < \alpha_2)$, we first note that for $|\varepsilon^*| \ll 1$ rad, $\Delta\alpha \approx \alpha - \alpha^*$ and $\Delta\varepsilon \approx \varepsilon - \varepsilon^*$. For a given $\Delta\alpha$, Eq. (16) yields

$$c\theta = \frac{\tan\Delta\alpha}{\tan\varepsilon_{\text{spec}}} \tag{18}$$

which presents two values of θ and therefore two values of the boundary angle ε for a given α yielding one $\Delta\varepsilon > 0$ and the other $\Delta\varepsilon < 0$. Deducing $\sin\theta$ from Eq. (18), Eq. (17) furnishes

$$s\Delta\varepsilon = \pm\left[\sin^2\varepsilon_{\text{spec}} - \cos^2\varepsilon_{\text{spec}} \tan^2\Delta\alpha\right]^{\frac{1}{2}} \tag{19}$$

Between the two $\Delta\varepsilon$ that value is selected whose sign matches with the sign of the original $\Delta\varepsilon$ that will have slewed the boresight inside the disc. The new ε is finally calculated from $\varepsilon = \varepsilon^* + \Delta\varepsilon$, and the boresight is commanded to slide along the disc until the ε of the versine profile ceases to bring the boresight inside the disc anymore. While sliding along the disc perimeter, the slope $\mathrm{d}\varepsilon/\mathrm{d}\alpha$ is governed by

$$\frac{\mathrm{d}\varepsilon}{\mathrm{d}\alpha} = \frac{\cos\varepsilon^* \cos\varepsilon \sin(\alpha - \alpha^*)}{\sin\varepsilon^* \cos\varepsilon - \cos\varepsilon^* \sin\varepsilon \cos(\alpha - \alpha^*)} \tag{20}$$

III. Communication Maintenance of Pitch (y) and Yaw (z) Antennae

Figure 5 illustrates the beam cones of $-y$ (ultra high frequency) and $\pm z$ (low data rate) antennae. Only one of the two yaw antennae will be installed on the vehicle of interest, but, to keep the exclusion algorithm general, both antennae are considered in this study. If the vector from an antenna to the ground station is within the antenna's cone, the communication link is maintained, otherwise it is not. In the event of a communication outage, the communication is restored by a roll rotation β of the vehicle about the x axis (see Fig. 3 for transformations) because the axes of the antennae cones are along the pitch and yaw axes. The magnitude of this rotation is determined to be such that while the communication link is preserved for one antenna it is not lost for the other. This loss may inadvertently happen because the y and z antennae are mounted on orthogonal axes and signal strength for one antenna is made stronger at the expense of the other. It therefore seems logical to roll the vehicle incrementally, while the boresight (x axis) is slewing, so as to maintain the angle of the ground station with one of the z antennae equal to the angle with the $-y$ antenna. This roll motion is formulated next. Depending on the antenna characteristics, maintaining the two angles equally may not always be desired, but the assumption is made here that this is the desired goal.

A time-varying vehicle body frame $\bar{x}_b\ \bar{y}_b\ \bar{z}_b$, shown in Fig. 3, is arrived at after a rotation of (α, ε) formulated in Sec. II. The antennae in this orientation of the vehicle may or may not have a communication link with the ground. Our objective now is to determine a roll angle β that not only links the $-y$ antenna and either the $+z$ or $-z$ antenna with the ground, but equalizes as well the signal strengths of the two. Let $\boldsymbol{\rho}$ be a unit vector from the vehicle to the ground station (Fig. 5) with the components in the frame $\mathcal{F}^{\bar{b}}$: $\bar{x}_b\ \bar{y}_b\ \bar{z}_b$ as $\boldsymbol{\rho}\ \mathcal{F}^{\bar{b}} = [\bar{x}_b\ \ \bar{y}_b\ \ \bar{z}_b]^T$, where the superscript T means transpose. When the vehicle is rolled by an angle β about the axis $\bar{x}_b = x_b$, equalizing the signal strengths, the body frame $\mathcal{F}^b$: $x_b\ y_b\ z_b$ is arrived at. The components of $\boldsymbol{\rho}$ in this frame are $[x_b\ \ y_b\ \ z_b]^T$. Let ϕ_{+z}, or ϕ_z for short, be the angle between $+z$-antenna cone axis and $\boldsymbol{\rho}$; likewise, let ϕ_{-z} be the angle between $-z$-antenna cone axis and $\boldsymbol{\rho}$ and ϕ_{-y} between $-y$ axis and $\boldsymbol{\rho}$. Reference 8 then shows that for equal signal strengths for $+z$ and $-y$ antennae $(\phi_z = \phi_{-y})$ the required roll rotation β in terms of the components of $\boldsymbol{\rho}$ prior to β rotation is

$$+z \text{ antenna: } \tan\beta = \frac{\bar{y}_b + \bar{z}_b}{\bar{y}_b - \bar{z}_b} \tag{21}$$

and, after rotation,

$$\phi_{-y} = \phi_z = \cos^{-1}\left(1/\sqrt{2}\right)\left(1 - x_b^2\right)^{\frac{1}{2}} \tag{22}$$

One infers from Eq. (22) that for a given $\boldsymbol{\rho}$ vector, and therefore a given x_b component that does not change with rotation, the angle ϕ_{-y} $(=\phi_z)$ achieved after the roll is predetermined by $x_b = \bar{x}_b$ whether this establishes the communication link of the two antennae or not, that is, whether $\phi_{-y} = \phi_z$ is less than the semicone angle θ_{cone} or not, depending on the location of the ground station and attitude of the vehicle. A certain degree of mission planning is thus indicated. For the antennae along $-y$ axis and $-z$ axis, for $\phi_{-y} = \phi_{-z}$ the required roll angle β is[8]

$$-z \text{ antenna: } \tan\beta = \frac{-\bar{y}_b + \bar{z}_b}{\bar{y}_b + \bar{z}_b} \tag{23}$$

and, after the rotation β, $y_b = z_b$.

In actual implementation of the preceding algorithm, the angle β is not calculated for each sample relative to the frame $\bar{x}_b\ \bar{y}_b\ \bar{z}_b$. Instead, one calculates $\delta\beta$ rotation with respect to the frame $x_b\ y_b\ z_b$ of the preceding sample and then increment the preceding roll by $\delta\beta$ as the azimuth and elevation angles α and ε evolve. This action will maintain the same yaw antenna (either $+z$ or $-z$) throughout

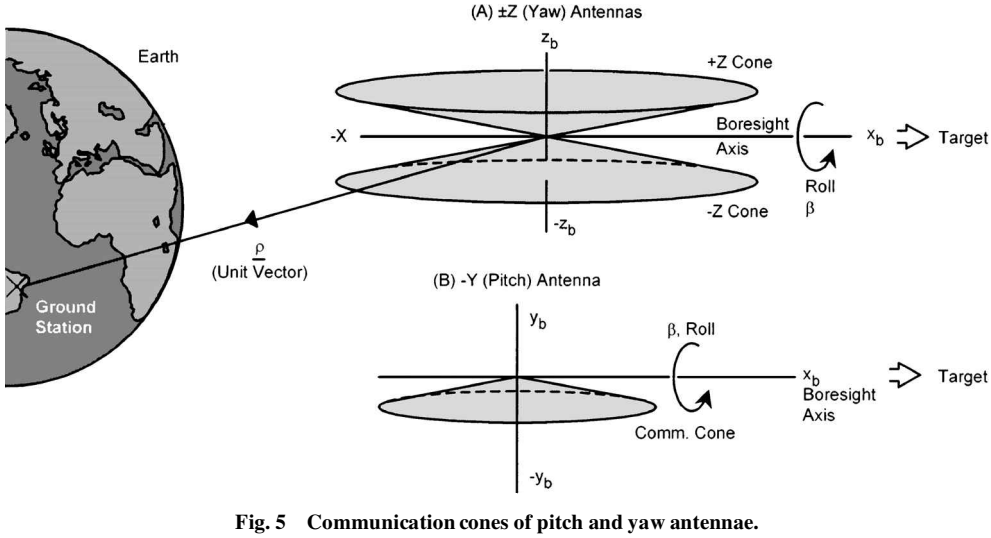

Fig. 5 Communication cones of pitch and yaw antennae.

the slew in link with the ground. Incidentally, if the ground is not in link before the slew is initiated, the link is established by rolling the vehicle in accordance with Eq. (21) or Eq. (23).

IV. Communication Maintenance of $-x$ Antenna

For the purposes of this study, the communication of the ground station with the $-x$ antenna (a high data rate antenna) and the pitch or yaw antenna (a low data rate antenna) is not concurrent. The objective now is to maintain the communication of the $-x$ antenna while the vehicle performs a pitch or yaw slew to steer the payload to view a star and then returns to reacquire the target. These slews may be required, for example, for updating navigation processes (for estimation of random walk of the gyros, for instance).

Let ϕ_{-x} be the angle between $\boldsymbol{\rho}$ and the antenna beam axis $-x_b$. The requirement for communication, then, is $\phi_{-x} \leq \theta_{\text{cone}}$ where θ_{cone} is the semicone angle of the $-x$ antenna beam. Because $\boldsymbol{\rho} \cdot (-\boldsymbol{b}_1) = \cos\phi_{-x}$, ($\boldsymbol{b}_1$ is the unit vector along the x_b axis) the just-stated requirement is equivalent to

$$\cos\phi_{-x} \geq \cos\theta_{\text{cone}} \tag{24}$$

In terms of the components of $\boldsymbol{\rho} = [x_b \;\; y_b \;\; z_b]^T$, the requirement (24) is the same as the following two constraints:

$$-x_b \geq \cos\theta_{\text{cone}} \tag{25}$$

$$y_b^2 + z_b^2 \leq \sin^2\theta_{\text{cone}} \tag{26}$$

Satisfaction of these constraints will now be examined in the context of a large pitch or yaw maneuver.

Pitch or Yaw Rotation of $+\pi/2$

Suppose, to reorient the thrusters for navigation update, the mission planning requires any of the four possible ± 90-deg rotations about the pitch and yaw axis of the vehicle. Of the four, that rotation is to be selected for which the ground station remains within the beamwidth of the $-x$ antenna throughout the rotation. Consider a pitch rotation of ϕ about the y_b axis. Let $[x_{b0} \;\; y_{b0} \;\; z_{b0}]^T$ be the unit vector to the ground station before rotation and $[x_{bf} \;\; y_{bf} \;\; z_{bf}]^T$ be the unit vector after rotation. For $\phi = \pi/2$, $[x_{bf} \;\; y_{bf} \;\; z_{bf}]^T = [-z_{b0} \;\; y_{b0} \;\; x_{b0}]$. Applying the inequality (25) to the initial and final x components, we obtain

$$\pi/2 \text{ pitch: } -x_{b0} \geq \cos\theta_{\text{cone}} \tag{27a}$$

$$z_{b0} \geq \cos\theta_{\text{cone}} \tag{27b}$$

If the initial ground-station unit vector satisfies these conditions, the station will remain in communication before, during, and after a 90-deg pitch rotation. For $\phi = -\pi/2$ rotation the requirement (25) leads to

$$-\pi/2 \text{ pitch: } z_{b0} \leq -\cos\theta_{\text{cone}} \tag{28}$$

From Eqs. (27) and (28) we conclude that, if the ground is in link with the vehicle before rotation, a $\pi/2$ y rotation is chosen if z_{b0} satisfies the condition (27b), and a $-\pi/2$ y rotation is chosen if z_{b0} satisfies the condition (28). If neither condition is satisfied, a rotation about the z_b axis, which we consider now, is then resorted to. Imposing the requirement (25) on x_b for $\phi = 0$ and $\pm\pi/2$ angle of rotation about the z_b axis, the following conditions emerge for maintaining communication before and after rotation:

Initially:

$$-x_{b0} \geq \cos\theta_{\text{cone}} \tag{29}$$

$\pi/2$ yaw:

$$-y_{b0} \geq \cos\theta_{\text{cone}} \tag{30}$$

$-\pi/2$ yaw:

$$y_{b0} \geq \cos\theta_{\text{cone}} \tag{31}$$

We infer from Eq. (30) that if the y_{b0} component of the initial ground-station unit vector meets this condition, then a $\pi/2$ rotation about the z_b axis is to be commanded, whereas if it satisfies the condition (31), a $-\pi/2$ rotation about the z_b axis is to be commanded.

Figure 6 illustrates the four constraints (27b), (28), (30), and (31) on the initial location of the ground-station projection in the communication cone of the $-x$ antenna. If the ground station is located

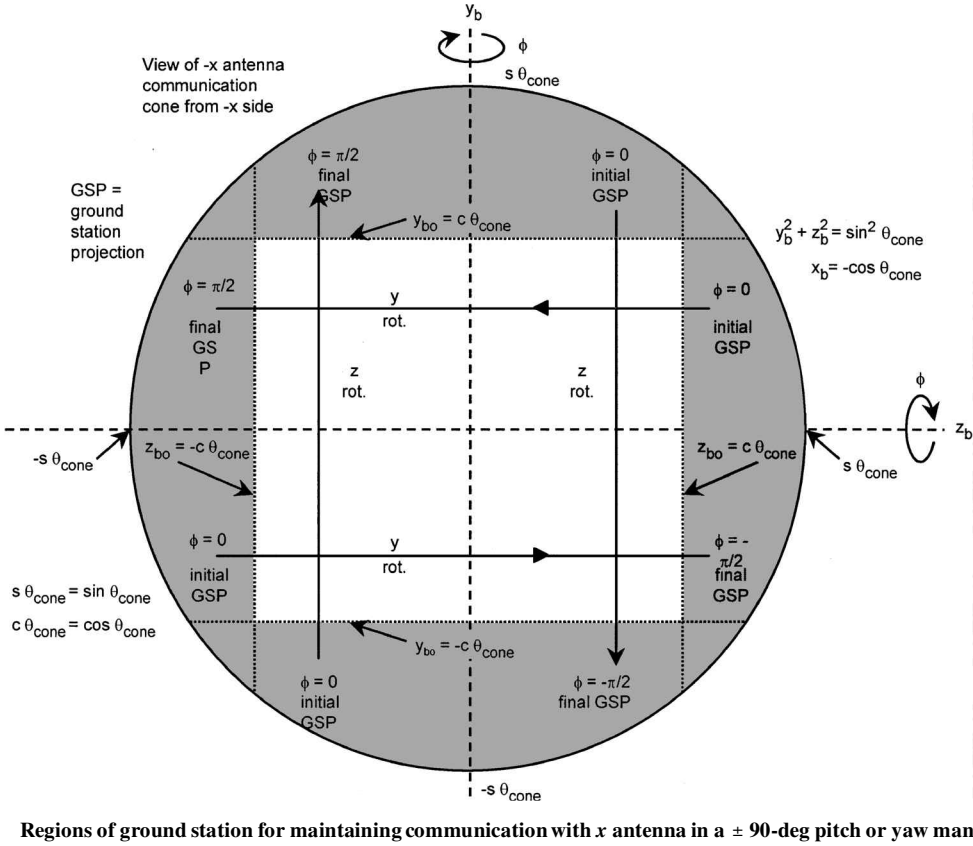

Fig. 6 Regions of ground station for maintaining communication with x antenna in a ± 90-deg pitch or yaw maneuver.

such that either $|y_{b0}| \geq c\theta_{\text{cone}}$ or $|z_{b0}| \geq c\theta_{\text{cone}}$, the communication will be preserved after a suitably chosen ±90-deg rotation about the y_b or z_b axis of the vehicle, as just determined. Figure 6 shows this by the four directions of travel of the ground-station image from its initial to final location within the cone. Also, these four constraints imply that if the initial ground unit vector is located such that $|y_{b0}| < c\theta_{\text{cone}}$ and $|z_{b0}| < c\theta_{\text{cone}}$—the unshaded square area concentric with the cone circle, the communication might be broken after a pitch or yaw 90-deg maneuver (see the following).

Forbidden Region of Ground-Station Projection in the Communication Cone of the $-x$ Antenna

If the ground station is initially within the cone and if $|y_{b0}| < c\theta_{\text{cone}}$ and $|z_{b0}| < c\theta_{\text{cone}}$ (Fig. 6), a 90-deg maneuver about the pitch or yaw will drive it outside the cone. Communication may still be restored by a roll motion before the pitch or yaw maneuver if the components y_{b0}, z_{b0} are such that this preroll motion brings the ground station within any of the four segments $|y_{b0}| > c\theta_{\text{cone}}$ and $|z_{b0}| > c\theta_{\text{cone}}$, that is, if the (y_{b0}, z_{b0}) point lies on a concentric circle of radius greater than the $c\theta_{\text{cone}}$. Figure 7 identifies these regions in shade. To formulate them, note that the square region $|y_{b0}| = c\theta_{\text{cone}}$ and $|z_{b0}| = c\theta_{\text{cone}}$ in Figs. 6 and 7 circumscribe a circle of radius $c\theta_{\text{cone}}$ governed by $y_b^2 + z_b^2 = \cos^2\theta_{\text{cone}}$, equivalent to $x_b = -\sin\theta_{\text{cone}}$ ($x_b < 0$ so that the ground station is within the $-x$ antenna). If the ground station is initially within this circle

Forbidden region:

$$y_{b0}^2 + z_{b0}^2 < c^2\theta_{\text{cone}} \quad \text{or} \quad -x_{b0} > \sin\theta_{\text{cone}} \tag{32}$$

a roll motion can never bring the ground station to the region $|y_b| > c\theta_{\text{cone}}$ or $|z_b| > c\theta_{\text{cone}}$, and hence the communication will not be restorable. The ground station, therefore, must not be in this forbidden region initially. In terms of the angle ϕ_{-x}, the forbidden circle (32) can be rewritten as

Forbidden region:

$$\cos\phi_{-x} > \sin\theta_{\text{cone}} \tag{33}$$

For example, for $\theta_{\text{cone}} = 60$ deg the ground station at $\phi_{-x} < 30$ deg will be in the forbidden region for an imminent 90-deg maneuver. This result appears obviously correct because if $\phi_{-x} < 30$ deg, a 90-deg maneuver in the opposite direction of the initial ϕ_{-x} will lead to a final $\phi_{-x} > (90 - 30) = 60$ deg outside the cone. We are thus led to the conclusion that if the ground station is initially within the shaded region of the cone shown in Fig. 7 a preroll motion will maintain communication even after the pitch/yaw maneuver.

Regarding the magnitude and direction of this preroll angle, denoted β, we first require that its magnitude be minimum. To achieve this, intuition suggests that if $|y_{b0}| < |z_{b0}|$ then β rotation should decrease $|y_{b0}|$ to zero. Likewise, if $|z_{b0}| < |y_{b0}|$, then β rotation should render $|z_{b0}|$ to zero. This rule keeps $|\beta| \leq 45$ deg. Following this rule, we arrive at

$$\begin{aligned} &\text{if} \quad |y_{b0}| < |z_{b0}|: \beta = \tan^{-1}(-y_{b0}/z_{b0}) \Rightarrow y_b = 0 \\ &\text{if} \quad |z_{b0}| \leq |y_{b0}|: \beta = \tan^{-1}(z_{b0}/y_{b0}) \Rightarrow z_b = 0 \end{aligned} \tag{34}$$

Thus, the vehicle is rolled by an angle β given by Eq. (34) first, and then it performs the multiaxis slew motion (α, ε). One can, of course, use instead an equivalent single rotation just as well.

V. Compatibility of Exclusion Motion with Communication Constraint

Figure 8 illustrates a large rotation α of the vehicle about the z_b' axis inclined at an angle γ (Fig. 3) from the z_b axis. Because of the positive α rotation, the ground station, which is on the $-x_b$ side so as to communicate with the $-x$ antenna, moves relatively in a direction parallel to the $+y_b'$ axis. On the other hand, the boresight axis x_b moves such that a bright object disc appears to move in the $-y_b'$ direction. Then, if the disc parameters are such that $\varepsilon_{\text{spec}} > |\varepsilon^*|$ (as in Fig. 8), the boresight axis x_b will see the bright object while turning about the z_b' axis. To avoid this, the vehicle is rotated by ε about the α-displaced y_b' axis. Because the sensor can pass the bright object tangentially from either side of the disc (points A and B in Fig. 8 and as illustrated in Figs. 1a and 1b), our objective now is to determine which of the two choices is consistent with the requirement of keeping the ground station within the communication cone, for we observe in Fig. 8 that the ε rotation can move the ground station either closer to the beam axis or farther from it and possibly out of the cone, depending on the sign ε.

From the sequence of transformations in Fig. 3 (without considering the roll angle β for $\pm z$ and y antenna), we obtain

$$\begin{aligned} x_b = {} & x_{b0}\, c\varepsilon\, c\alpha + y_{b0}\,(c\varepsilon\, s\alpha\, c\gamma + s\varepsilon\, s\gamma) \\ & + z_{b0}\,(c\varepsilon\, s\alpha\, s\gamma - s\varepsilon\, c\gamma) = -\cos\phi_{-x} \end{aligned} \tag{35}$$

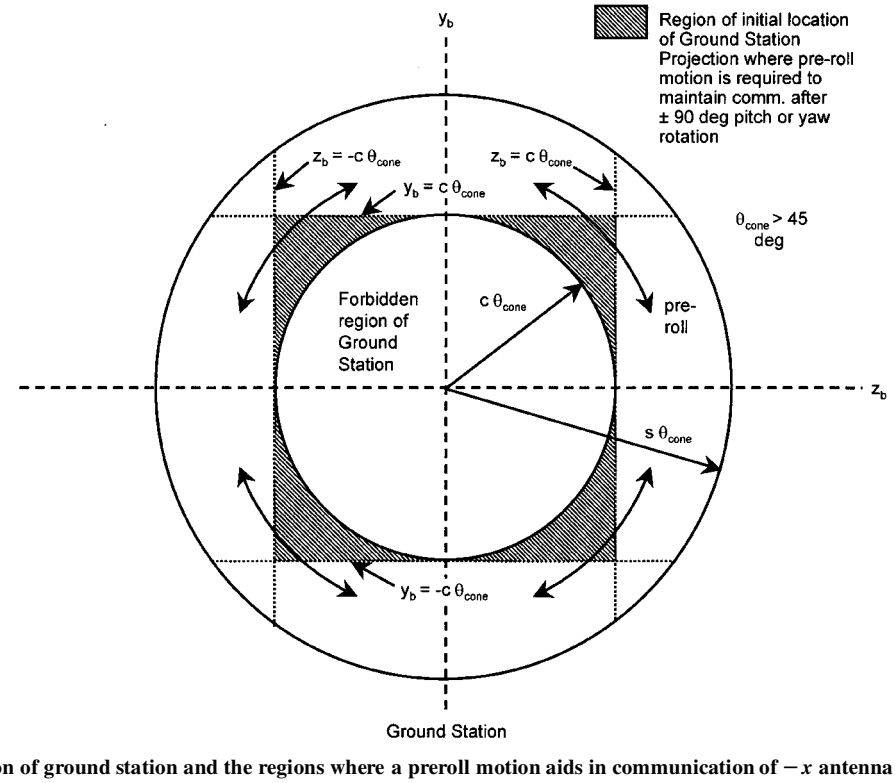

Fig. 7 Forbidden region of ground station and the regions where a preroll motion aids in communication of $-x$ antenna after a ± 90-deg pitch or yaw rotation.

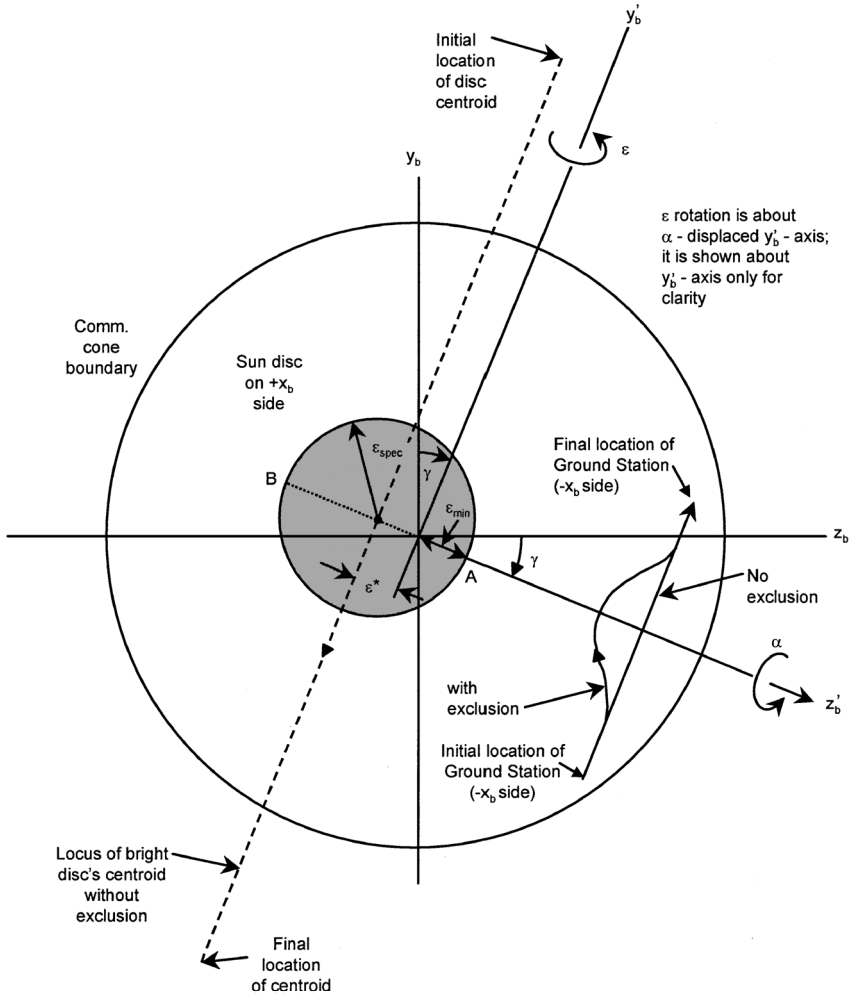

Fig. 8 Motion of ground station in the communication cone of $-x$ antenna and the motion of a bright object relative to the sensor along $+x$ side of the vehicle.

where, as before, x_{b0}, y_{b0}, z_{b0} are the components of the initial ground unit vector. To determine the ε that decreases ϕ_{-x} ($\partial\phi_{-x} < 0$) so that the ground station moves toward the cone axis, we differentiate Eq. (37) with respect to ε and evaluate the derivative at $\varepsilon = 0$, arriving at

$$\left.\frac{\partial\phi_{-x}}{\partial\varepsilon}\right|_{\varepsilon=0} = -\frac{z'_{b0}}{\sin\phi_{-x}} \tag{36}$$

where z'_{b0} is the component of the ground-station unit vector along the axis of rotation z'_{b0} before the rotation. The slope is evaluated at $\varepsilon = 0$ because we intend to decrease ϕ_{-x} relative to its ideal value corresponding to $\varepsilon = 0$ for a complete range of ε including its zero initial value. Initially, because $0 \le \phi_{-x} \le \theta_{\text{cone}} < \pi/2$, $\sin\phi_{-x} \ge 0$, and therefore the requirement $\partial\phi_{-x} < 0$ leads to the condition $z'_{b0}\ \partial\varepsilon > 0$, which gives the following rule for selecting the sign of exclusion motion

$$\text{sign}(z'_{b0}) = \text{sign}(\varepsilon) \tag{37}$$

Also note that if the exclusion motion is not required at all (that is, $\varepsilon = 0$ for the complete range of maneuver α), z'_{b0} will not be changed by α because α is the angle of rotation about z'_{b0}. Finally, we note that the condition (37) is invoked just once to determine the sign of ε for a given bright object provided $|z'_{b0}|$ is greater than some small number, say 0.1, below which the ground station is assumed to be already so close to the cone axis that ε motion of either sign would not push it outside the cone.

As an illustration, apply the condition (37) to a situation depicted in Fig. 8 where $z'_{b0} > 0$, implying that $\varepsilon > 0$. Notice that according to the sign convention of counterclockwise positive ε^* is positive in Fig. 8, and therefore the avoidance angle ε for this bright disc must be $\varepsilon = \varepsilon^* + \varepsilon_{\text{spec}} > 0$. If the communication constraint were absent, the minimum avoidance angle $\varepsilon_{\min} = -\varepsilon_{\text{spec}} + \varepsilon^* < 0$ would have sufficed. The influence of communication constraint on the exclusion motion is thus apparent.

VI. Angular-Rate Commands for Large-Angle Maneuvers

When the vehicle is commanded to perform simultaneously the ideal slew α, the exclusion motion ε, and the roll motion β for maintaining communication with $\pm z$ and $-y$ antennae, according to the transformations shown in Fig. 3 the associated rate commands in the instantaneous, commanded body frame are found to be

$$\omega_{c1} = -\dot\alpha\sin\varepsilon + \dot\beta \tag{38a}$$

$$\omega_{c2} = \dot\alpha\cos\varepsilon\sin(\beta-\gamma) + \dot\varepsilon\cos(\beta-\gamma) \tag{38b}$$

$$\omega_{c3} = \dot\alpha\cos\varepsilon\cos(\beta-\gamma) - \dot\varepsilon\sin(\beta-\gamma) \tag{38c}$$

If the vehicle is commanded to preroll to maintain communication of the $-x$ antenna (without α and ε rotations), the commanded rate of rotations will then be $\omega_{c1} = \dot\beta$ and $\omega_{c2} = 0 = \omega_{c3}$.

VII. Illustrations

While developing the preceding exclusion-communication algorithm, we applied it to innumerable scenarios, from simplest to most complex, including a Monte Carlo simulation in which the sun was located randomly in a celestial sphere, equivalent to specifying an arbitrary initial attitude of the vehicle. In the following we present one

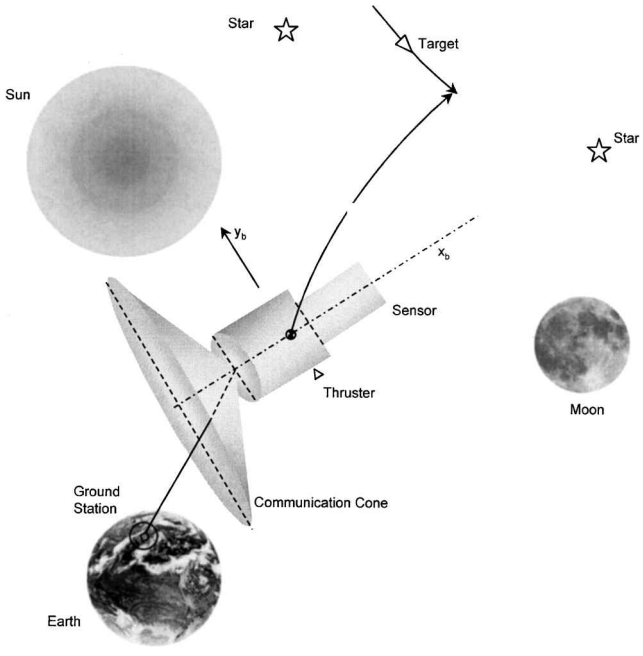

Fig. 9 A vehicle to be maneuvered avoiding the sun, moon, and Earth, and maintaining communication with the ground station.

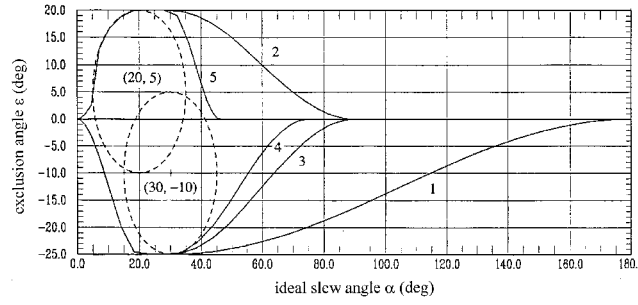

Fig. 10 Avoidance of overlapping sun and moon in a multislew scenario: deviated slew paths.

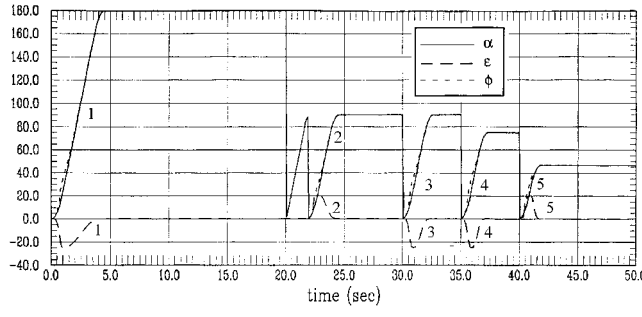

Fig. 11 Ideal slew angle α, exclusion angle ε, and equivalent single-axis rotation angle ϕ vs time.

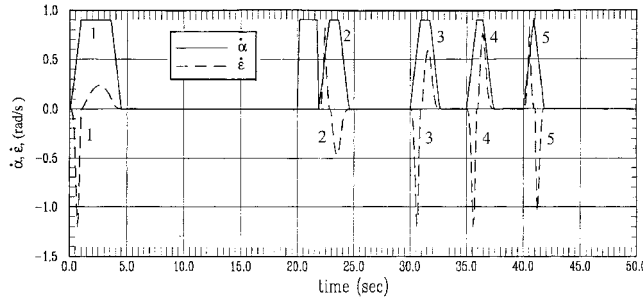

Fig. 12 Ideal slew rate $\dot{\alpha}$ and exclusion rate $\dot{\varepsilon}$ vs time.

of the worst-case stressing scenarios simulated. Consider a vehicle in a near-Earth ballistic trajectory (Fig. 9). En route it performs five different large-angle maneuvers, avoiding sun, moon, and Earth, and maintaining communication with the ground station. Figures 10–13 illustrate these maneuvers, the associated commands, avoidance of bright objects, and maintenance of communication. Sun and moon locations are hypothetical. The moon's phases are ignored, and it is considered to be full bright regardless of its location relative to the sun. This assumption is not tenable, but it allows us to illustrate the versatility of the algorithm. The centroids of sun and moon are placed at $\alpha^* = 20$ deg, $\varepsilon^* = 5$ deg, and $\alpha^* = 30$ deg, $\varepsilon^* = -10$ deg, respectively, relative to each slew plane. The forbidden angular radius $\varepsilon_{\text{spec}}$ around each bright object is taken to be 15 deg, and therefore the minimum exclusion angle is -10 deg for the sun and 5 deg for the moon. Each large-angle maneuver is followed by a tracking or attitude hold phase for a short duration. The maneuvers are 1) a 180-deg pitch, after separation from the launch vehicle, to point the sensor in the expected direction of a target; 2) a 90-deg yaw to align a particular thruster in the LOS direction; 3) a 90-deg pitch/yaw to align the sensor with Star-1 for gyro calibration; 4) a perpendicular 75-deg pitch/yaw to view Star-2; and 5) a 45-deg pitch/yaw to point the boresight in a desired direction. Figure 10 illustrates the avoidance of the sun and moon in the α-ε plane. Two special features of this example are that 1) the two bright discs overlap so much that they cover each other's ε_{min} tangent point at respective α^* and 2) the first object is so close to the initial orientation of the sensor ($\alpha^* = 20$ deg, whereas $\varepsilon_{\text{spec}} = 15$ deg) that the versine ε profile enters this disc. As such, and also because of the communication requirements, the modified centroidal exclusion angles ε in Fig. 10 for both $\alpha^* = 20$ and 30 deg, for every maneuver, are not equal to their minimum values. Furthermore, because the versine ε profile for the maneuvers 2 and 5 enter the first bright disc for some range of $\alpha < \alpha^*$, the versine profile is replaced by the bright disc perimeter where necessary so that the sensor glides around the disc. The time-fuel optimal profiles of α and corresponding $\varepsilon(\alpha)$ profiles, partly versine and partly along the disc perimeter, vs time are illustrated in Fig. 11. The unnumbered 90-deg maneuver in Fig. 11 is a roll motion for selecting a particular thruster. The angle ϕ in this figure is the single-axis equivalent of (α, ε). The slew rates $\dot{\alpha}$ and $\dot{\varepsilon}$ are displayed in Fig. 12, $\dot{\alpha}$ as a time/fuel optimal profile and $\dot{\varepsilon} = \dot{\alpha}\, d\varepsilon/d\alpha$. The slope discontinuity in ε vs α profile at the point where $\varepsilon(\alpha)$ versine profile enters the disc and the variation of ε around the disc perimeter cause rapid variations in $d\varepsilon/d\alpha$ and hence in $\dot{\varepsilon}$. Figure 13 portrays the communication establishment first and then its maintenance for the $-x$ antenna. It shows a 60-deg circular boundary of the conical beam and a 30-deg boundary of the forbidden region of the ground station, as portrayed earlier in Fig. 6. Prior to the first 180-deg pitch rotation, the $-z$ antenna is in link with the ground station, and the $-x$ antenna is not. As the rotation progresses, the ground station leaves the beam of $-z$ antenna and enters the $-x$ antenna beam; this is depicted in Fig. 13 by the entry of the ground-station unit vector into the $-x$ antenna cone. From then on, the ground-station trace remains within the conical beam during all of the maneuvers.

In the absence of exclusion motion, a pitch/yaw rotation causes the ground-station trace in the yz plane of the vehicle to move in a straight line perpendicular to the axis of rotation, and a roll motion produces a circular arc trace. With the perpendicular exclusion motion the ground-station trace becomes sinuous. This is implicit in Figs. 6 and 8 and is illustrated in Fig. 13. The requirement of communication maintenance imposes $\varepsilon < 0$ for acquiring the stars and $\varepsilon > 0$ to point the boresight in the final desired direction. As a result, the corresponding straight traces have wriggled toward the beam center in Fig. 13. On the other hand, the signs of ε for a 180-deg pitch and a 90-deg yaw (the maneuvers 1 and 2) are not influenced by this requirement because the corresponding traces start from $y_b = 0$ and $z_b = 0$, respectively.

The commanded motions just illustrated are multiaxis, formulated in terms of three large angles: slew angle, exclusion angle, and roll angle for communication, giving rise to a time-varying commanded transformation matrix for the flight controller to follow. Singularity-free quaternion commands are derived from the transformation

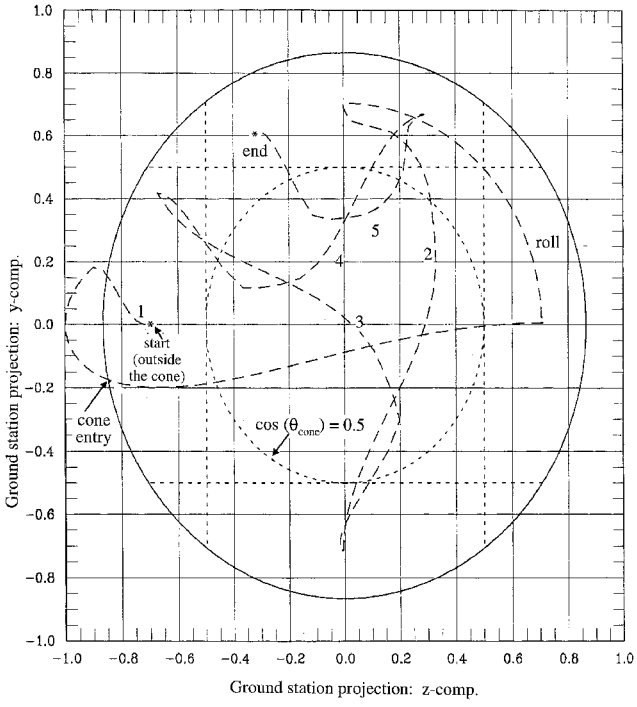

Fig. 13 Motion of ground-station projection in the communication cone of $-x$ antenna during large-angle maneuvers and small-angle tracking: y comp. vs z-comp.

matrix and inputted to the flight controller. The quaternion commands and the corresponding angular rate commands in the commanded body frame are shown in Ref. 9. To maneuver the vehicle, both the quaternion commands and the rate commands are fed to a three-axis attitude controller such as one for Hubble Space Telescope[10] or interplanetary spacecraft Viking[11] using thrusters and phase plane control logic.

VIII. Conclusions

In the preceding, a general formulation is presented to determine if a seeker focal plane will encounter, while changing its direction in space, a bright object, and a general multi-axis avoidance path is developed so that the seeker optics remains away from the radiant object by at least the specified angle. These angular and rate commands are time-varying and, compared to step commands, they are time- and fuel-efficient. At any time during slew if the sensitive seeker is about to enter the forbidden angular disc around a bright object centroid, the algorithm presented commands the seeker boresight to slide along the disc perimeter instead, protecting the expensive seeker focal plane. Whereas this motion is about the pitch and yaw axes of the vehicle, the algorithm includes an additional motion, about roll axis, to simultaneously maintain communication of ground station with the vehicle's antenna. The sign of the bright object avoidance motion is selected such that the ground-station projection in the communication cone moves toward the cone axis and not to the cone surface. The algorithm is well-illustrated with a realistic stressing scenario of a space vehicle.

To apply this algorithm in flight, it is accompanied with the sun and moon ephemeredes, time-varying inertial location of the ground station, trajectory of the vehicle, the desired direction of its boresight in J2000 frame, and the initial inertial attitude of the vehicle. The resulting time-varying attitude commands are multi-axis, effecting the desired slew of a vehicle sensor from one direction to other, swerving the sensor away from a hot source if it is in the way, and rolling the vehicle to maintain communication of the antennae with the ground. Because of the versatility of the algorithm, the flight software to generate the attitude and rate commands for all phases of flight is relatively long. It can be shortened somewhat, though, by combining the preroll motion for communication maintenance of the $-x$ antenna with the slew and exclusion motion, effecting an equivalent rotation; by considering only one bright object (sun) instead of the sun, moon, and Earth; and by enlarging the forbidden perimeter of the bright disc and not insisting on sliding along the perimeter in case the boresight enters an outer annular region of the enlarged disc. Whereas this abridged version of the algorithm may be accommodated on a flight computer, the original version may be used for mission planning on ground.

Acknowledgments

Technical discussions with D. Pearson, M. Rivera, and M. Nakano, lending considerable insight into the exclusion-communication problem investigated here, are gratefully acknowledged. The step command approach sketched in the Introduction is credited to B. Nguyen.

References

[1]Guldner, J., and Utkin, V. I., "Sliding Mode Control for Gradient Tracking and Robot Navigation Using Artificial Potential Fields," *IEEE Transactions on Robotics and Automation*, Vol. 11, No. 2, 1995, pp. 247–254.

[2]McInnes, C. R., "Large Angle Slew Maneuvers with Autonomous Sun Vector Avoidance," *Journal of Guidance, Control, and Dynamics*, Vol. 17, No. 4, 1994, pp. 875–877.

[3]McInnes, C. R., "Potential Function Methods for Autonomous Spacecraft Guidance and Control," *Advances in the Astronautical Sciences*, Univelt, Inc., San Diego, CA, Vol. 90, Paper AAS 95-447, 1996, pp. 2093–2109.

[4]McInnes, C. R., "Nonlinear Control for Large Angle Attitude Slew Maneuvers," *Proceedings of the Third ESA Symposium on Spacecraft Guidance, Navigation, and Control*, European Space Research and Technology Centre, Noordwijk, The Netherlands, 1996, pp. 543–548.

[5]Sorenson, A. M., "ISO Attitude Maneuver Strategies," American Astronautical Society, Paper AAS 93-317, 1993, pp. 975–987.

[6]Singh, G., Macala, G., Wong, E., and Rasmussen, R., "A Constraint Monitor Algorithm for the Cassini Spacecraft," *Proceedings of the AIAA Guidance, Navigation, and Control Conference*, AIAA, Reston, VA, 1997, pp. 272–282.

[7]Frakes, J. P., Henretty, D. A., Flatley, T. W., Markley, F. L., San, J. K., and Lightsey, E. G., "SAMPEX Science Pointing with Velocity Avoidance," *AAS/AIAA Spaceflight Mechanics Meeting*, AAS Paper 92-182, 1992, pp. 949–966.

[8]Hablani, H. B., "Spacecraft Slews Avoiding Celestial Objects and Maintaining Communication with Ground Station," NASA CP-3345, May 1997.

[9]Hablani, H. B., "Attitude Commands Avoiding Bright Objects and Maintaining Communications with Ground Station," NASA CP-1998-206858, May 1998.

[10]Glaese, J. R., Kennel, H. F., Nurre, G. S., Seltzer, S. M., and Shelton, H. L., "Low-Cost Space Telescope Pointing Control System," *Journal of Spacecraft and Rockets*, Vol. 13, No. 7, 1976, pp. 400–405.

[11]Holmberg, N. A., Faust, R. P., and Holt, H. M., *Viking '75 Spacecraft Design and Summary, Vol. 1—Lander Design*, NASA Ref. Publication 1027, 1980.